Orbital orderings and optical conductivity of SrRuO$_3$ and CaRuO$_3$: first-principles studies

Orbital orderings and optical conductivity of SrRuO₃ and CaRuO₃: first-principles studies

Guang-Tao Wang[1,2], Min-Ping Zhang[1], Zong-Xian Yang[1] and Zhong Fang[2]

[1] Department of Physics, Henan Normal University, Xinxiang, Henan 453007, People's Republic of China
[2] Beijing National Laboratory for Condensed Matter Physics, and Institute of Physics, Chinese Academy of Sciences, Beijing 100190, People's Republic of China

Abstract
The Jahn–Teller (JT) distortion induced orbital order and optical conductivity in SrRuO₃ and CaRuO₃ are investigated by first-principles calculations. The total energy and optical conductivity of all the spin ordering states of SrRuO₃ and CaRuO₃ are calculated in the LDA + U scheme with $U_{\text{eff}} = 2.5$ eV. The down-spin t_{2g} of Ru show antiferromagnetic-like orbital order in the a–b plane. We observe a d–d transition peak at an energy of about 1.0 eV in the calculated optical conductivity and analyze the reason for it not being observed in previous experiments.

(Some figures in this article are in colour only in the electronic version)

1. Introduction

Orbital order related properties of transition-metal oxides (TMOs) [1–5] have been interesting topics for physical and material scientists in recent years due to the strong couplings among the spin, lattice and charge degrees of freedom in these compounds. The direct observation of orbital structure is difficult, yet several experiments [6–9] have been developed to detect the anisotropy induced by spin and orbital orderings. Among them, the measurement of anisotropic optical conductivity [8, 9] by using polarized light could provide us with some useful information. The low energy (<3 eV) optical excitations (mostly come from the transition-metal d–d transitions) are able to reflect sensitively the orbital orderings for d electrons in TMOs.

Generally, 4d orbitals are more extended than 3d orbitals in TMOs. So, the hybridization of 2p–4d is more important than that of 2p–3d. Although the 4d orbitals are more extended and the correlation effect is weaker than that of 3d electrons, some measurements such as thermal, magnetic, transport properties [10, 11], photoemission [12–14] and optical conductivity spectroscopy [15–18] of SrRuO₃ and CaRuO₃ have shown that the electron correlation effects in the Ru 4d are important.

Both SrRuO₃ and CaRuO₃ are in the *Pbnm* orthorhombic unit cell with $a \approx b \approx c/\sqrt{2}$, including four formula units per cell [19, 20]. There are four 4d electrons per Ru⁴⁺ site. Synchrotron x-ray and neutron diffraction results [19, 20] have shown that there are JT distortions in the octahedron of SrRuO₃ and CaRuO₃, leading to the split-off degenerated energy level of t_{2g}. So the four electrons of Ru⁴⁺ will occupy t_{2g} orbitals selectively and orderly, which will induce spin ordering. SrRuO₃ has been known as a bad metal, showing a ferromagnetic ordering at Curie temperature (T_C) ∼ 160 K. CaRuO₃ is also barely metallic, but its magnetic ground state remains enigmatic to date and is still the subject of controversy: Goodenough [21] believed that it was antiferromagnetic; Yoshimura [22] observed robust ferromagnetic spin fluctuations in CaRuO₃ and argued that it was exchange enhanced paramagnetic; Mukuda [23], by means of nuclear magnetic resonance (NMR), demonstrated that it was nearly a ferromagnetic (FM) metal; Felner [24] using Mössbauer studies and Kolev [25] using Raman spectroscopy found it was a spin glass with short range magnetic interaction.

In order to clarify these controversies, we calculated the total energy and optical conductivity of different magnetic states (FM, A, C, G-type antiferromagnetic), where FM denotes ferromagnetic, A-type represents ferromagnetic in the

a–*b* plane but antiferromagnetic along the *c* axis, C-type marks ferromagnetic along the *c* axis, but antiferromagnetic in the *a*–*b* plane, G-type means antiferromagnetic both in the *a*–*b* plane and along the *c* axis [3, 26]. We appropriately decouple the spin degree of freedom and treat it in terms of the Heisenberg model, then the exchange interaction is estimated by mapping the calculated total energies of each magnetic state [27] to the Heisenberg model. So, the nearest neighboring exchange coupling constants are given by

$$J_c = -[E(\text{F}) - E(\text{G}) - E(\text{A}) + E(\text{C})]/(4S^2)$$

$$J_{ab} = -[E(\text{F}) - E(\text{G}) + E(\text{A}) - E(\text{C})]/(8S^2)$$

where $E(\text{F})$, $E(\text{A})$, $E(\text{C})$ and $E(\text{G})$ are the total energy of ferromagnetic, A, C, G-type antiferromagnetic respectively and $S = 1$ is the moment. The calculated results are compared with experimental measurements.

2. Method and details

Total energies and optical properties of $SrRuO_3$ and $CaRuO_3$ are studied by the first-principles plane-wave basis pseudopotential calculations in the BJSTATE code [3]. The 4d states of Ru and 2p states of O are treated with the ultrasoft pseudopotentials [28] and the other states by the optimized norm-conserving pseudopotentials [29]. All the pseudopotentials used in this study have been well checked [4, 5]. The inter-band optical conductivity is calculated from the converged Kohn–Sham wavefunctions $|\psi_{n\mathbf{k}}\rangle$ and eigenvalues $E_n(\mathbf{k})$ by the Kubo formula [30, 31]. Generally speaking, correlation effects are believed to be less important in describing 4d TMOs than 3d ones, because 4d electrons are more delocalized than 3d electrons. However, recent reports [10–18] on $SrRuO_3$ and $CaRuO_3$ showed that the correlation effect might play an important role in determining their physical properties. So we used the LDA + *U* method [32, 33] in the calculation. This method is proposed by Anisimov [32] and implemented in the plane-wave pseudopotentials scheme by Sawada [33]. In the LDA + *U* method the choice of localized orbitals is very important because U_{eff} is applied on such orbitals. However, ambiguity exists in the choice of localized orbitals, especially in the case of using the plane-wave basis method. For those methods based on the local basis like LMTO (linear-muffin-tin orbital), it is natural to use the basis orbitals as the localized orbitals. However, in the plane-wave basis method, the definition of localized orbital is nontrivial. Following the idea of Sawada [33], a truncated pseudo-atomic wavefunction is chosen as the localized orbital to which U_{eff} is applied. The other crucial problem in the practical LDA + *U* calculations is the choice of U_{eff}. Generally two ways are followed to estimate U_{eff}. First, U_{eff} can be directly calculated by using the constrained local density approximation (LDA) method. However, it is not so meaningful to take this approach in the plane-wave method because of some arbitrariness in the definition of localized orbitals. The second way is to adjust U_{eff} so as to fit the calculated band gap with an experimental one.

It is well known that density functional theory (DFT) is bad at calculating band gaps, especially for TMOs. So the LDA + *U* method was proposed to reproduce band gaps by adjusting parameter *U*. Here we use $U = 3.5$ eV and $J = 1.0$ eV ($U_{\text{eff}} = 2.5$ eV) to reproduce experimental band gaps. Such a parameter has been checked as a suitable parameter by our previous work [5] and by Jeng [34]. The cut-off energy for describing the wavefunctions is 36 Ryd, while that for the augmentation charge is 200 Ryd. And we used a $(10 \times 10 \times 8)$ mesh for the *k*-points in the linear tetrahedron method with the curvature correction.

The unit cell and coordinates are defined the same as in figure 1 of [34]. We defined the *x*, *y* and *z* axes as the $[1\bar{1}0]$, [110] and [001] directions of the unit cell, respectively. Four Ru atoms are defined as $Ru^1(0.0, 0.0, 0.0)$ and $Ru^2(0.5, 0.5, 0.0)$ in the first layer, $Ru^3(0.0, 0.0, 0.5)$ and $Ru^4(0.5, 0.5, 0.5)$ in the second layer. The oxygen atoms in the *a*–*b* plane are denoted as O^2; at the apex of the RuO_6 octahedra, the oxygen atoms are named as O^1.

3. Results and discussion

Figure 1 shows the partial density of state (PDOS) of Ru1 and Ru2 in $SrRuO_3$. In the ionic model, the four 4d electrons of Ru occupy the low energy level of t_{2g} ($t_{2g}^3\uparrow$, $t_{2g}^1\downarrow$), keeping the high energy level of e_g empty. There are JT distortions in the *a*–*b* plane as well as rotation and zig-zag tilting of RuO_6 octahedra along the *c*(*z*) axis. For the $SrRuO_3$, the distance between Ru^1 and O^2 along the *x* axis is $Ru^1O^2(x) = 2.038$ Å and along the *y* axis is $Ru^1O^2(y) = 1.942$ Å. The distance between Ru^1 and O^1 along the *z* axis is $Ru^1O^1(z) = 1.979$ Å. Because of the JT distortion and rotation of RuO_6 octahedra, the degenerated energy level of $t_{2g}^1\downarrow$ of Ru^1 will split as $E_{yz} > E_{xy} > E_{zx}$, where E_{yz}, E_{xy} and E_{zx} are the energy levels of d_{yz}, d_{xy} and d_{zx} orbitals respectively. So the down-spin electron of $t_{2g}^1\downarrow$ will preferentially occupy the $d_{zx}\downarrow$ state; however, the split is too small for the $d_{zx}\downarrow$ state to be fully occupied, leaving d_{yz} and d_{xy} orbitals empty. As a result, the three out of four electrons of Ru^1 will occupy the $d_{xy/yz/zx}\uparrow$, and the other one will partially occupy $d_{zx}\downarrow$ and $d_{xy}\downarrow$ to lower its energy. On the other hand, $Ru^2O^2(x) = 1.942$ Å, $Ru^2O^2(y) = 2.038$ Å, $Ru^2O^1(z) = 1.979$ Å, $t_{2g}^3\downarrow$ will split as $E_{zx} > E_{xy} > E_{yz}$, so the down-spin of Ru^2 will partially occupy $d_{zy}\downarrow$ and $d_{xy}\downarrow$. For $t_{2g}^3\downarrow$ of Ru^1, the occupation numbers are $n_{xy} = 0.45$ and $n_{zx} = 0.52$. As for Ru^2, the occupation numbers are $n_{xy} = 0.45$, $n_{yz} = 0.52$. Ru^1 and Ru^3 have the same orbital order, while Ru^1 and Ru^2 have zig-zag orbital ordering. So the C-type orbital order (antiferromagnetism-like in the *a*–*b* plane and ferromagnetism-like along the *c* axis) is formed.

The PDOS of Ru1 and Ru2 in the $CaRuO_3$ are revealed in figure 2. Similarly with $SrRuO_3$, it has the FM spin order and C-type-like orbital order. The JT distortion is different from that of $SrRuO_3$ as follows: $Ru^1O^2(x) = 2.028$ Å, $Ru^1O^2(y) = 1.981$ Å, $Ru^1O^1(z) = 1.981$ Å, $Ru^2O^2(x) = 1.981$ Å, $Ru^2O^2(y) = 2.028$ Å, $Ru^2O^1(z) = 1.981$ Å. Because $Ru^1O^2(x)$ is larger than the other bonds, the electrons favor partially occupying $d_{zx}\downarrow$ and $d_{xy}\downarrow$ in Ru^1. For the same reason, the electrons favor partially occupying $d_{zy}\downarrow$ and $d_{xy}\downarrow$ in Ru^2.
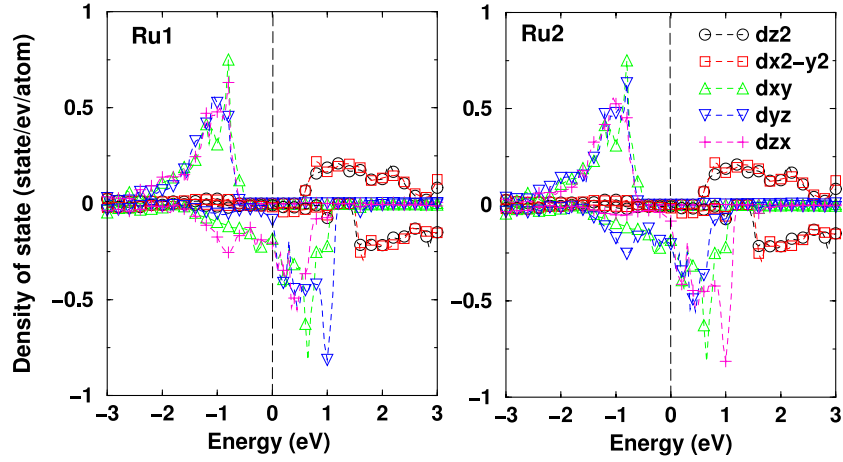
Figure 1. PDOS of Ru1 (left) and Ru2 (right) in SrRuO$_3$ with $U = 2.5$ eV. Different orbitals are labeled by different colors and symbols. (black and circle: d$_{z^2}$, red and square: d$_{x^2-y^2}$, green and triangle up: d$_{xy}$, blue and triangle down: d$_{yz}$, magenta and plus: d$_{zx}$).
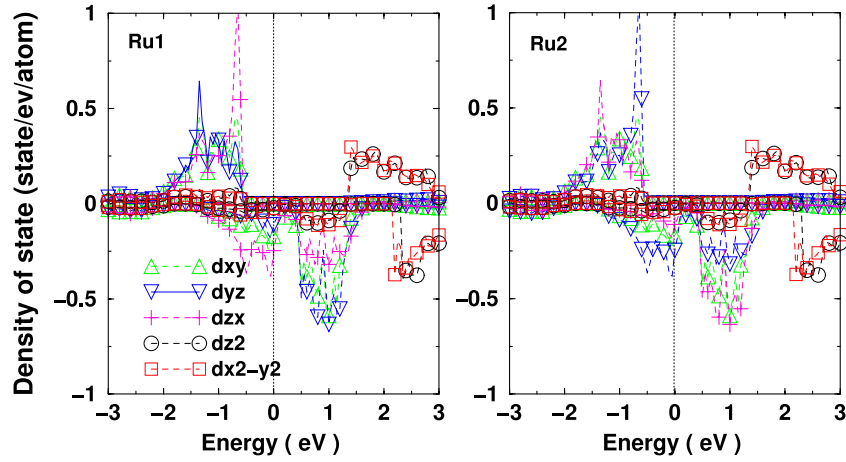
Figure 2. PDOS of Ru1 (left) and Ru2 (right) in CaRuO$_3$ with $U = 2.5$ eV. Different orbitals are labeled by different colors and symbols. (black and circle: d$_{z^2}$, red and square: d$_{x^2-y^2}$, green and triangle up: d$_{xy}$, blue and triangle down: d$_{yz}$, magenta and addition symbol: d$_{zx}$).

Table 1. The relative energies per unit cell of NM (non-magnetic), FM, A-, C- and G-type antiferromagnetism and the exchange constant calculated with the Heisenberg model [31] (in the unit of meV).

Sample	U (eV)	NM	FM	A	C	G	J_{ab}	J_c
SrRuO$_3$	2.5	421.63	0	63.73	106.50	64.80	13.4	5.5
CaRuO$_3$	2.5	371.6	0	19.3	24.1	18.5	2.91	3.4

The angle ∠Ru^{1}O^{2}Ru^2 is 147.01 in CaRuO$_3$, while it is 161.09 in SrRuO$_3$. The angle ∠Ru^{1}O^{2}Ru^3 is 149.61 in CaRuO$_3$, while it is 164.94 in SrRuO$_3$. Comparing the bond angle between SrRuO$_3$ and CaRuO$_3$ we find the rotation and tilt angles of the RuO$_6$ in CaRuO$_3$ are bigger than those in SrRuO$_3$. It must be noted that the only structural difference between the Sr- and Ca-based compounds is the rotating and tilting degrees of RuO$_6$, which are a bit larger in the latter due to the smaller size of Ca^{2+} compared with Sr^{2+}. The occupied numbers of Ru^1 are $n_{xy} = 0.41$ and $n_{zx} = 0.55$. As for Ru^2, the occupied number are $n_{zx} = 0.41$ and $n_{yz} = 0.55$.

The relative energies per unit cell are presented in table 1, where $E(F)$, $E(A)$, $E(C)$ and $E(G)$ represent energies per unit cell for FM, A-, C- and G-type antiferromagnetism,

respectively. We mapped the calculation results to the Heisenberg model to get the exchange constant. For both SrRuO$_3$ and CaRuO$_3$, the total energy of FM is the smallest and the exchange constants of J_{ab} and J_c are positive, which indicates that the ground state is FM. The exchange constant of CaRuO$_3$ is smaller than that of SrRuO$_3$. This might due to the rotation and tilt angle of the RuO$_6$ octahedron of CaRuO$_3$ is bigger than that of SrRuO$_3$. The increased rotation and tilt angle of CaRuO$_3$ reduces the exchange integration. The small exchange constant is one of the characteristics of the spin glass [18]. In such a compound, the exchange constant is too small to form long range magnetic order, which agrees well with the spin glass state proposed by Felner [18] and Goodenough [21]. For SrRuO$_3$, J_{ab} is larger than J_c, which
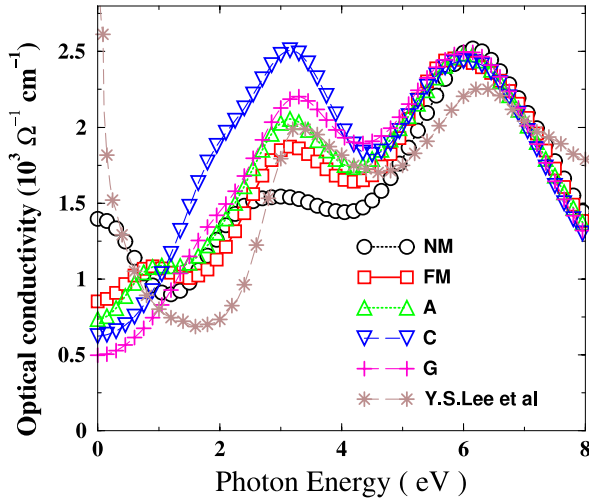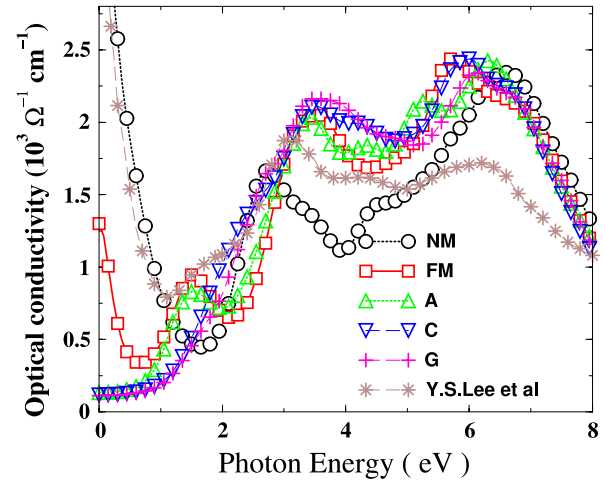
Figure 3. The optical conductivity of SrRuO$_3$ in the spin state of NM, FM, A, C, G and experimental results of Lee.

Figure 4. The optical conductivity of CaRuO$_3$ in the spin state of NM, FM, A, C, G and experimental results of Lee.

may result in the spin order being more likely to form in the *a–b* plane because the exchange integration between Ru^1 and Ru^2 is larger than that between Ru^1 and Ru$_3$. Furthermore it may explain why the easy magnetic axis [11] is [100] or [010] rather than [001]. For CaRuO$_3$, $J_{ab} < J_c$, so the exchange integration between Ru^1 and Ru$_3$ is larger than that between Ru^1 and Ru^2, which means the easy axis is more likely to be along [001]. Such results are confirmed by Felner's [24] experiments.

It is well known that both LDA and the generalized gradient approximation (GGA) exaggerate magnetic tendency. So it is difficult to calculate an exact value of T_C from the exchange coupling J. However, the calculated exchange coupling J is proportional to the Curie temperature T_C. Because the exchange J of SrRuO$_3$ is much larger than that of CaRuO$_3$, the former is FM below T_C (about 160 K), while the latter shows spin glass behavior [18, 35]. Such a significant difference in exchange constant between SrRuO$_3$ and CaRuO$_3$ comes from the difference of rotation and tilt angle of the RuO$_6$ octahedron.

Figures 3 and 4 show the calculated optical conductivity of SrRuO$_3$ and CaRuO$_3$ in the spin states of NM, FM, A, C and G, comparing them with the experimental results of Lee [17] and Lee [16]. In figure 3, two peaks appear at 3.0 and 6.0 eV, which come from the electron transitions from occupied O 2p to unoccupied t$_{2g}$ and e$_g$ states of Ru respectively [16]. From figures 1 and 2, we can see that the energy split between e$_g$ and t$_{2g}$ is about 3.0 eV. Above 2.0 eV, our calculated optical conductivity is coincident with Lee's [16] experiments with SrRuO$_3$. For CaRuO$_3$, even above 2.0 eV, there is some discrepancy between the calculated and experimental optical conductivity. Such a discrepancy maybe derived from the 'strain effect' [16] in the sample. The sample used in the optical conductivity measurement was epitaxially grown on the SrTiO$_3$ substrates [16]. So the lattice mismatch induced a 'strain effect', which changed the transport properties of CaRuO$_3$ significantly [16, 36]. Below 2.0 eV there are some differences for both SrRuO$_3$ and CaRuO$_3$: for FM and A-type antiferromagnetism, there is a peak at an energy of about

1.0 eV, resulting from the transition from the partially occupied t$_{2g}\downarrow$ of Ru^1 to the unoccupied t$_{2g}\downarrow$ of Ru^2. This peak has been predicted and observed by Ahn [15] in the films of SrRuO$_3$ and CaRuO$_3$. They explained this peak as electrons translated from the QP (quasi-particle) band to the UHB (upper Hubbard band), which will cost energy of as much as $U/2$. Why did not Lee *et al* observe the lower energy peak? We thought the reason might be that they did the experiment at *room-temperature* (300 K), but the Curie temperature T_C is about 160 K. Above T_C the thermal vibration breaks the spin ordering, so the FM order and the d–d transition channels are destroyed. If the FM spin order remained in the *a–b* plane, the electrons of Ru^1 could hop from d$_{xy}\downarrow$ to Ru^{2}d$_{xy}\downarrow$. However, if it is antiferromagnetic in the *a–b* plane, when electrons hop from d$_{xy}\downarrow$ of Ru^1 to d$_{xy}\uparrow$ of Ru^2, they have to invert their spin direction, which rarely happens. So the electron–phonon interaction breaks the spin order and simultaneously impedes the d–d transition. Figure 4 displays a similar optical conductivity pattern to figure 3. We predicted that if the optical conductivity of SrRuO$_3$ could be measured at low temperature (below T_c), the d–d transition at an energy of about 1.0 eV might be observed.

4. Conclusion

In this paper, we have discussed JT distortion induced orbital order in SrRuO$_3$ and CaRuO$_3$. We calculated the total energy and optical conductivity of all the spin ordering states (NM, FM, A-, C-, G-type antiferromagnetism) of SrRuO$_3$ and CaRuO$_3$ in the LDA + U scheme with $U_{\text{eff}} = 2.5$ eV. From the energy difference in CaRuO$_3$ between different magnetic states, we predicted that CaRuO$_3$ prefers to take the spin glass state. Mapping the total energy to the Heiseng model, we gave the exchange constant as follows: for SrRuO$_3$, $J_{ab} = 13.4$ and $J_c = 5.5$; for CaRuO$_3$, $J_{ab} = 2.9$ and $J_c = 3.4$. Comparing our calculated optical conductivity results with the experimental data of [16, 17], we suggested the reason they did not observe the low energy d–d transition peak in the

optical conductivity might be that the experiment was done at room temperature. At such a high temperature, the thermal vibration would have destroyed the FM magnetic order, which is important for the d–d transition. If they had measured the optical conductivity of SrRuO$_3$ at low temperature (below T_c), they might have observed the d–d transition at an energy of about 1.0 eV.

Acknowledgments

References

[1] Tokura Y and Nagaosa N 2000 *Science* **288** 462
[2] Fang Z, Solovyev I V and Terakura K 2000 *Phys. Rev. Lett.* **84** 3169
[3] Fang Z and Terakura K 2002 *J. Phys.: Condens. Matter* **14** 3001
[4] Jung J H, Fang Z, He J P, Kaneko Y, Okimoto Y and Tokura Y 2003 *Phys. Rev. Lett.* **91** 56403
[5] Fang Z, Nagaos N and Terakura K 2004 *Phys. Rev. B* **69** 45116
[6] Murakami Y, Hill J P, Gibbs D, Blume M, Koyama I, Tanaka M, Kawata H, Arima T, Tokura Y, Hirota K and Endoh Y 1998 *Phys. Rev. Lett.* **81** 582
[7] Saitoh E, Okamoto S, Takahashi K T, Tobe K, Yamamoto K, Kimura T, Ishihara S, Maekawa S and Tokura Y 2001 *Nature* **410** 180
[8] Okimoto Y, Tomioka Y, Onose Y, Otsuka Y and Tokura Y 1999 *Phys. Rev. B* **59** 7401
[9] Tobe K, Kimura T, Okimoto Y and Tokura K 2001 *Phys. Rev. B* **64** 184421
[10] Allen P B, Berger H, Chauvet O, Forro L, Jarlborg T, Junod A, Revaz B and Santi G 1996 *Phys. Rev. B* **53** 4393
[11] Cao G, McCall S, Shepard M, Crow J E and Guertin R P 1997 *Phys. Rev. B* **56** 321
[12] Okamoto J, Mizokawa T, Fujimori A, Hase I, Nohara M, Takagi H, Takeda Y and Takano M 1999 *Phys. Rev. B* **60** 2281
[13] Park J, Oh S-J, Park J-H, Kim D M and Eom C-B 2004 *Phys. Rev. B* **69** 085108
[14] Kim J, Chung J and Oh S-J 2005 *Phys. Rev. B* **71** 121406
[15] Ahn J S, Bak J, Choi H S, Noh T W, Han J E, Bang Y, Cho J H and Jia Q X 1999 *Phys. Rev. Lett.* **82** 5321
[16] Lee J S, Lee Y S, Noh T W, Char K, Park J, Oh S-J, Park J-H, Eom C B, Takeda T and Kanno R 2001 *Phys. Rev. B* **64** 245107
[17] Lee Y S, Lee J S, Noh T W, Young Byun D, Soo Yoo K, Yamaura K and Takayama-Muromachi E 2003 *Phys. Rev. B* **67** 113101
[18] Vidya R, Ravindran P, Kjekshus A, Fjellvag H and Hauback B C 2004 *J. Solid State Chem.* **177** 146
[19] Zayak A T, Huang X, Neato J B and Rabe K M 2006 *Phys. Rev. B* **74** 094104
[20] Shikano M, Huang T-K, Inaguma Y, Itoh M and Nakamura T 1994 *Solid State Commun.* **90** 115
[21] Longo J M, Raccah P M and Goodenough J B 1968 *J. Appl. Phys.* **39** 1327
[22] Yoshimura K, Imai T, Kiyama T, Thurber K R, Hunt A W and Kosuge K 1999 *Phys. Rev. Lett.* **83** 4397
[23] Mukuda H, Ishida K, Kitaoka Y, Asayama K, Kanno R and Takano M 1999 *Phys. Rev. B* **60** 12279
[24] Felner I, Nowik I, Bradaric I and Gospodinov M 2000 *Phys. Rev. B* **62** 11332
[25] Kolev N, Chen C L, Gospodinov M, Bontchev R P, Popov V N, Litvinchuk A P, Abrashev M V, Hadjiev V G and Iliev M N 2002 *Phys. Rev. B* **66** 014101
[26] Imada M, Fujimori A and Tokura Y 1998 *Rev. Mod. Phys.* **70** 1039
[27] Fang Z and Nagaosa N 1999 *Phys. Rev. Lett.* **93** 176404
[28] Vanderbilt D 1990 *Phys. Rev. B* **41** 7892
[29] Vanderbilt D 1985 *Phys. Rev. B* **32** 8412
[30] Wang C S and Callaway J 1974 *Phys. Rev. B* **9** 4897
[31] Fang Z, Nagaosa N and Terakura K 2003 *Phys. Rev. B* **67** 035101
[32] Anisimov V I, Zaanen J and Anderson O K 1991 *Phys. Rev. B* **44** 943
Anisimov V I, Solovyev I V, Korotin M A, Czyzyk M T and Sawatzky G A 1993 *Phys. Rev. B* **48** 16929
Solovyev I V, Dederichs P H and Anisimov V I 1994 *Phys. Rev. B* **50** 16 861
Liechtenstein A I, Anisimov V I and Zaanen J 1995 *Phys. Rev. B* **52** R5467
Anisimov V I, Aryasetiawan F and Liechtenstein A I 1997 *J. Phys.: Condens. Matter* **9** 767
[33] Sawada H, Morikawa Y, Terakura K and Hamada N 1997 *Phys. Rev. B* **56** 12154
[34] Jeng H-T, Lin S-H and Hsue C-S 2006 *Phys. Rev. Lett.* **97** 67002
[35] Rado G T 1963 *Magnetism* (New York: Academic) pp 67–8
[36] Rao R A, Gan Q, Cava R J, Suzuki Y, Gausepohl S C, Lee M and Eom C B 1997 *Appl. Phys. Lett.* **70** 3035